

ABSTRACT

POPPO, MICHAEL NICHOLAS. Dynamic Simulation of Walking with a Passive Elastic Ankle Exoskeleton and the Effects of the Underlying Plantarflexor Muscle Tendon Unit Neuromechanics. (Under the direction of Katherine Saul).

Recent breakthroughs in exoskeleton walking devices have been shown to decrease the metabolic cost of walking by up to 7% using a clutch-spring mechanism aimed at reducing the load requirements of the plantarflexors during stance (Collins, Wiggin et al. 2015). This was the first passive device to perform this feat. Joint-level analysis revealed that this whole-body metabolic reduction was achieved in a “sweet spot” of stiffness, but it is unclear why this occurs. To investigate potential causes of this “sweet spot,” a simple model of an “exo-tendon” in parallel with a lumped uniarticular plantarflexor muscle was employed (Sawicki and Khan 2015). This simulation revealed that higher spring stiffnesses unloaded the compliant biological muscle-tendon unit (MTU) as designed but the muscle fascicle experienced larger excursions. During instances of high stiffness, the muscle fascicles operated at points well above optimal fiber length reducing their ability to produce force, effectively detuning them. Ankle kinematics in this simulation were assumed to be constant with respect to unassisted walking although it is known that users of this device alter their gait during assisted walking. The purpose of the current investigation is to use a multi-joint model and experimental data driven simulation to further explore the muscle mechanics, dynamics, and energetics that lead to improved metabolic efficiency during assisted walking.

A subset of data collected from a previous study (Collins, Wiggin et al. 2015), including four healthy adults walking in the exoskeleton with no spring (“no spring”; $0 \text{ N}\cdot\text{m}\cdot\text{rad}^{-1}$), and walking in the exoskeleton at the optimal spring stiffness (“spring”; $180 \text{ N}\cdot\text{m}\cdot\text{rad}^{-1}$). A lower limb model was adapted and scaled to run experimental muscle activation driven forward

simulations. The resultant muscle states were used in an energetics model and mechanical and energetic states were analyzed. Underlying plantarflexor muscles were expected to require less metabolic energy during assisted walking despite operating at detuned muscle dynamics.

The addition of the spring reduced the muscle-generated ankle moments and altered the ankle kinematics to operate in a more plantarflexed state. This was associated with reduced force production and activation of the SOL and MG during assisted walking. Exoskeleton assistance effectively unloaded the muscle-tendon units causing increased operating fiber lengths for the SOL and MG during stance. The average force generation ability of the plantarflexors did not substantially change during stance despite an increase in average operating fiber length. Metabolic energy consumption of the SOL and MG were reduced with spring assistance but the LG consumed more metabolic energy during the spring condition. The LG generally resulted in opposite effects compared to the SOL and MG. Total metabolic consumption of the plantarflexors decreased during the spring assistance.

Average operating fiber length of the plantarflexors shifted towards the descending limb of the force-length relationship. This shift may have played a part in altering kinematics during assisted walking due to associated instabilities and injury avoidance. The unloaded ankle muscle-tendon units consumed less metabolic energy under the well-tuned spring condition. This reduction does not account for the whole-body metabolic efficiency previously reported (Collins, Wiggin et al. 2015) suggesting that proximal joint energetics are also linked to ankle assistance which is consistent with previous research (Mooney and Herr 2016, Uchida, Seth et al. 2016). The biarticular gastrocnemius heads react to ankle assistance in opposite ways despite their similar geometry suggesting that these muscles may play different roles during walking.

© Copyright 2017 Michael Nicholas Poppo

All Rights Reserved

Dynamic Simulation of Walking with a Passive Elastic Ankle Exoskeleton and the Effects of
the Underlying Plantarflexor Muscle Tendon Unit Neuromechanics

by
Michael Nicholas Poppo

A thesis submitted to the Graduate Faculty of
North Carolina State University
in partial fulfillment of the
requirements for the degree of
Master of Science

Mechanical Engineering

Raleigh, North Carolina

2017

APPROVED BY:

Dr. Andre Mazzoleni

Dr. Gregory Sawicki

Dr. Katherine Saul
Chair of Advisory Committee

BIOGRAPHY

As an engineer and athlete, I have always been interested in pushing the boundaries of human capabilities. Understanding current limitations is the first step to finding ways to tackle these obstacles. Technologies such as prosthetics and exoskeletons provide a unique opportunity to explore these boundaries and have the potential to augment human capabilities.

After receiving my Bachelors of Science in May 2015, I found a home conducting research in the Movement Biomechanics Laboratory under the direction the direction of Dr. Katherine Saul while pursuing my Masters of Science in Mechanical Engineering. My graduate research focused on understanding the effects external assistive devices have on underlying muscle mechanics and energetics during cyclic gaits using modeling and simulation techniques.

ACKNOWLEDGMENTS

First and foremost, I would like to thank my advisor, Dr. Katherine Saul. I cannot thank Dr. Saul enough for the support and guidance she has provided me over the past two years. I was honored to be part of her lab and to have the opportunity to work with and learn from her biomechanical and simulation experience. Dr. Saul's dedication and passion have pushed me to become a better engineer and researcher and I could not have achieved as much without her encouragement.

I would also like to thank Dr. Gregory Sawicki without whom this project would not have been possible. His insight and guidance was crucial to the analysis of the overall project, as well as my growth as a biomechanical engineer.

I would also like to thank Dr. Andre Mazzoleni for the support and motivation he provided me when I first began my graduate career. His graduate dynamics course provided me the strong background in mechanics that was crucial in evaluating results presented in this project.

I would like to give special thanks to Dr. Dominic Farris, Dr. Taylor Dick, and Emily McCain who were invaluable resources for me in conducting the simulation and analyzing data during this project. Dr. Dominic Farris provided significant assistance in implementing the simulation framework that he previously developed in addition to greatly expanding my knowledge of the inner workings of OpenSim models and simulation. Dr. Taylor Dick provided vital insight into the collection and evaluation of raw data including EMG, motion capture, and force plate ground reaction forces as well as insight into evaluating gait characteristics. Emily McCain provided valuable support and organization throughout this

process as well as providing critical assistance in generating visual and written data presentation.

I would also like to thank all my committee members and project contributors for the time and effort they have put into reviewing my research.

TABLE OF CONTENTS

LIST OF TABLES	vi
LIST OF FIGURES	vii
CHAPTER 1: INTRODUCTION	1
CHAPTER 2: METHODS	5
2.1 Data Acquisition and Post Processing	5
2.2 Model Development	8
2.3 Simulation	9
2.4 Analysis	10
CHAPTER 3: RESULTS	12
3.1 Joint-level Verification and Results	12
3.2 Muscle-level Results	14
CHAPTER 4: DISCUSSION	19
4.1 Summary	19
4.2 Discussion	19
4.3 Limitations	22
CHAPTER 5: CONCLUSION	25
5.1 Conclusion	25
5.2 Future Work	25
REFERENCES	27
APPENDIX	32

LIST OF TABLES

Table 1: Muscle parameters for base model before subject-specific scaling.....	8
Table A1: Average normalized fiber length for no spring condition.....	33
Table A2: Average normalized fiber length for spring condition.....	33
Table A3: Average activation for no spring condition	33
Table A4: Average activation for spring condition	34
Table A5: Average metabolic cost for no spring condition	34
Table A6: Average metabolic cost for spring condition	34
Table A7: Average normalized fiber force for no spring condition	35
Table A8: Average normalized fiber force for spring condition	35
Table A9: Average force generation ability for no spring condition	35
Table A10: Average force generation ability for spring condition	36

LIST OF FIGURES

Figure 2.1: Gain tuning ankle dynamics comparisons.....	7
Figure 3.1: Simulated ankle kinematics, dynamics, and power.....	12
Figure 3.2: Average ankle dynamics verification.....	13
Figure 3.3: Altered ankle kinematics.....	14
Figure 3.4: Normalized ankle plantarflexor force.....	15
Figure 3.5: Activation of plantarflexor muscles.....	16
Figure 3.6: Force generation ability of plantarflexor muscles.....	16
Figure 3.7: Normalized fiber length of plantarflexor muscles.....	17
Figure 3.8: Metabolic energy consumption.....	18

CHAPTER 1: INTRODUCTION

Walking is an essential daily activity that is required to participate in society, maintain independence, and maintain a positive quality of life. Walking is a well-tuned and relatively low cost form of locomotion that is the most common activity of daily living (Knaggs, Larkin et al. 2011). The metabolic demand of walking can be increased by additional factors such as load carriage or disease. For example, people with locomotor impairments as a result of stroke or spinal cord injury often experience significantly higher walking costs (Platts, Rafferty et al. 2006). Additionally, with increased aging, decreased preferred walking speed and increased metabolic costs are observed (Martin, Rothstein et al. 1992). Increased metabolic costs of walking results in muscle fatigue which can limit mobility (Westerterp 2013). For these reasons, both impaired and healthy individuals would benefit from reduced metabolic cost.

Exoskeletons are wearable passive or active devices that act in parallel with the human musculoskeletal system, and have the potential to augment or restore locomotor ability. For individuals with increased mechanical demands caused by disease-associated muscle weakness or load carrying, exoskeletons can be particularly helpful. Exoskeleton devices have application in rehabilitation (Banala, Kim et al. 2009), energy harvesting (Donelan, Li et al. 2008), and commercial and military uses (Gregorczyk, Hasselquist et al. 2010) and can be applied to various forms of locomotion including hopping (Grabowski and Herr 2009, Farris and Sawicki 2012, Farris, Robertson et al. 2013), running (Elliott, Sawicki et al. 2013, Cherry, Kota et al. 2016), and walking (Malcolm, Derave et al. 2013, Collins, Wiggin

et al. 2015). Prior work has shown that exoskeleton use can increase the preferred walking speeds of users and generate electrical power (Norris, Granata et al. 2007, Donelan, Li et al. 2008). Some exoskeletons have been able to reduce the metabolic cost of walking using active powered assistance (Mooney, Rouse et al. 2014, Mooney and Herr 2016). Unfortunately, powered exoskeletons are often low portability, increased weight, and higher cost.

Metabolic expenditure when using passive exoskeleton devices has typically exceeded unassisted normal walking (van Dijk, van der Kooij et al. 2011). However, a recent breakthrough in passive ankle exoskeletons has been shown to successfully reduce whole body metabolic cost of walking (Collins, Wiggin et al. 2015). This passive exoskeleton employed a simple clutch-spring mechanism in parallel with the ankle plantarflexors to unload the underlying muscle-tendon units. Joint-level analysis revealed that a 7% reduction in metabolic cost occurred in a “sweet spot” of exoskeleton stiffness, for which walking economy increased and muscle activity decreased.

Simple models of exoskeleton assistance predict unloading the muscle-tendon units may cause muscle mechanics to become detuned when working in parallel with an elastic “exo-tendon” (Sawicki and Khan 2015). In instances of high assistance during this simulation, muscle fiber lengths operated at points well into the descending limb of the force-length relationship which reduces the muscles ability to produce force. In a simulation of idealized exoskeleton assistance, models revealed that assisting a single joint such as the ankle during walking can have effects on non-

assisted degrees of freedom (Uchida, Seth et al. 2016). These models do not use experimental data and are simplified in that they assume that kinematics do not change with assistance; however, they are useful for providing insight into possible explanations for these observed effects. A recent study analyzed the energetics and joint-level mechanics of a bilateral, battery-powered ankle exoskeleton that reduced the metabolic cost of walking (Mooney and Herr 2016). This study showed that assisting the ankle during walking reduces positive mechanical work at the ankle, knee, and hip joints and that assistance results in augmented ankle moment and power.

One group has generated experimental data-driven muscle-level simulations of assisted walking using a work-based analysis approach to interpret results (Jackson, Dembia et al. 2017). This simulation reported that the soleus is required to generate more positive work during net-zero work assistance to the ankle and that summed muscle-generated energetics closely follow whole-body metabolic trends. Despite employing a model with muscles crossing the hip, knee, and ankle, an in-depth analysis of biarticular muscle mechanics was not performed. The accomplishment of the clutch-spring passive ankle exoskeleton is exceptional, however the underlying reason for the “sweet spot” remains unclear. Muscle-level analysis of experimental data is required to understand the impact of altered ankle kinematics and individual muscle contributions on plantarflexor mechanics and energetics during exoskeleton-assisted gait.

To address this knowledge gap, we employed a multi-joint model to drive forward simulations with experimental data and investigated the muscle-level impact

of exoskeleton-assisted walking in the stiffness “sweet spot.” We hypothesized that the metabolic improvement occurs when the underlying muscle dynamics are not shifted enough to elicit unfavorable mechanical conditions allowing the benefits of reduced muscle force requirements to reduce muscle-level metabolic cost. We expect decreased force generation ability of the ankle plantarflexors due to increased operating fiber lengths, but that these fiber dynamics will be accompanied by decreased muscle activation leading to overall reduced plantarflexors metabolic cost.

CHAPTER 2: METHODS

2.1 Data Acquisition and Post Processing

A subset of data collected from a previous study (Collins, Wiggin et al. 2015), including four healthy adults (N=4, 2 female, 2 male; age = 21.8 ± 2.5 yrs.; mass = 67.8 ± 2.1 kg; height = 1.76 ± 0.12 m; mean \pm s.d.) walking ($1.25 \text{ m}\cdot\text{s}^{-1}$) at two conditions was analyzed. The two conditions were: (1) walking in the exoskeleton with no spring (“no spring”; $0 \text{ N}\cdot\text{m}\cdot\text{rad}^{-1}$), and (2) walking in the exoskeleton at the experimental stiffness “sweet spot” (“spring”; $180 \text{ N}\cdot\text{m}\cdot\text{rad}^{-1}$). Subjects were allowed three seven-minute learning sessions for each condition before data was collected in the final two minutes of an additional seven-minute walking session. Each subject also performed a standing trial with and without the exoskeleton device on.

An eight-camera motion capture system was used to record the three-dimensional positions of 35 reflective markers during walking (Vicon, Oxford, UK). Ground reaction force data were collected from a split belt treadmill instrumented with load cells (Bertec, Columbus, OH, USA). Both motion capture and ground reaction force data were sampled at 120 Hz. Surface electromyography (EMG) of the soleus (SOL), medial and lateral gastrocnemii (MG and LG), and tibialis anterior (TA) were recorded at 960 Hz (SX230, Biometrics Ltd., Newport, UK).

All data was processed using OpenSim version 3.3 (Delp, Anderson et al. 2007) and Matlab R2016a (MathWorks, Natick, Massachusetts). Raw EMG data were processed using custom Matlab scripts that rectified, filtered (fourth order band pass filter between 20 and 300 Hz), and enveloped (rolling root mean square with a

window of 100 milliseconds) the signal. Because EMG data from maximum voluntary contraction (MVC) was unavailable, a subject-specific scale factor was applied to the EMG activation envelope. This scale factor was applied to the activation envelope for all muscles and conditions for each subject to approximate the appropriate activation of the muscles. This gain value was adjusted such that the summed muscle moment produced from forward dynamic simulations during no exoskeleton walking minimized RMS errors when compared to the joint-level ankle moment from inverse dynamics during mid stance (Fig 2.1). The “good” tuning is a good example because we decided to tune based on minimizing mid stance RMS error. The poor matching in terms of peak is ok because only about 83% of the summed plantarflexor PCSA is represented in the model (SOL MG LG). Maximum isometric forces of the muscles in the model were increased using a uniform gain for one subject due to the saturation of activation before the inverse and forward solutions agreed.

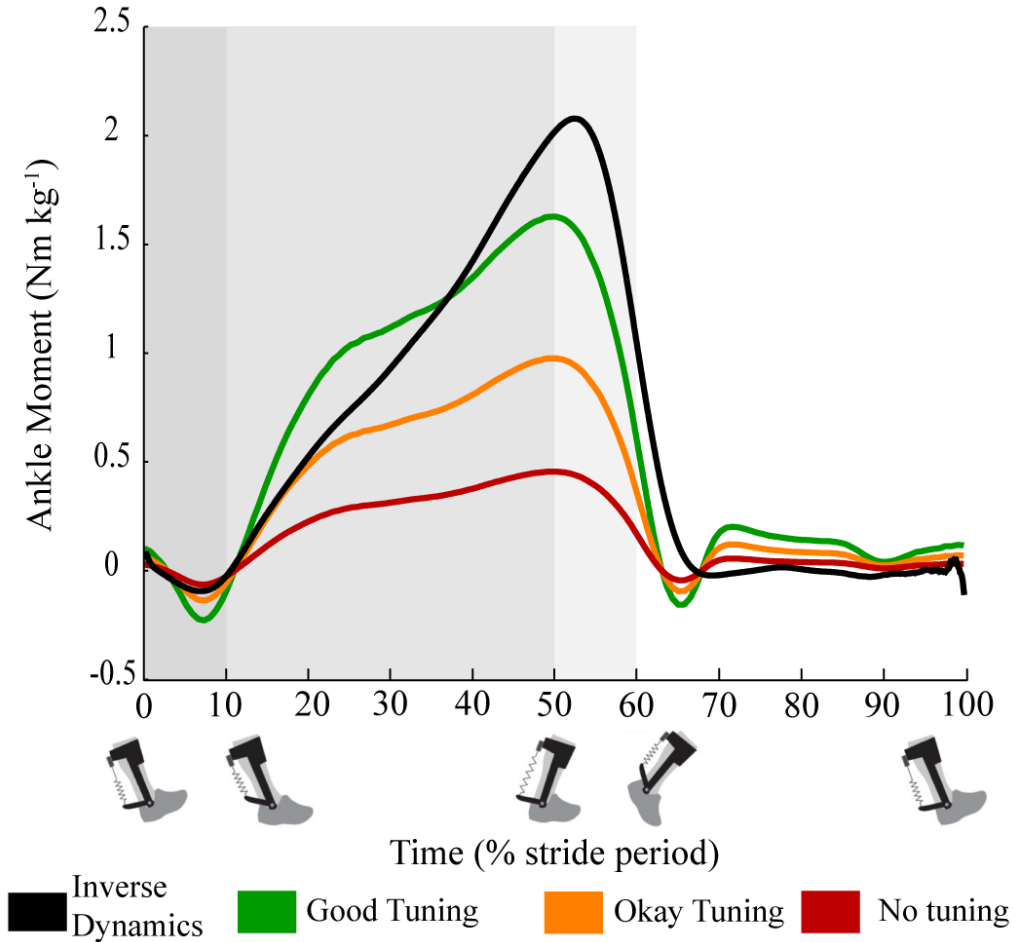


Figure 2.1: Gain tuning ankle dynamics comparisons

Comparing inverse dynamics to forward summed muscle moments (Nm kg⁻¹) for gain tuning against percent stride represented from 0-100%. Percent stride is broken down into swing (60-100% stride) and stance (0-60%). Stance phase is further broken down into early (0-10%), mid (10-50%), and late (50-60%) stance. Inverse dynamic solution (black line) compared to summed muscle moments about the ankle when no EMG gain tuning (red), okay EMG gain tuning (orange), and good EMG gain tuning (green) is used to drive the forward simulation.

2.2 Model Development

A lower limb model (Arnold, Ward et al. 2010) was adapted by removing all muscles except the SOL, MG, LG, and TA and adding a metabolic probe (Umberger, Gerritsen et al. 2003, Umberger 2010). Muscle parameters were also set based on average parameters from literature (Table 1). The ankle metatarsophalangeal and subtalar joints were also locked. SOL, MG, and LG were modeled with individual tendons as opposed to a single shared tendon as is physiological.

Table 1: Muscle parameters for base model before subject-specific scaling

	MG	LG	SOL	TA	Source
F_{\max} (N)	1308	606.4	3585.9	674	(Arnold, Ward et al. 2010)
V_{\max} ($L_0 s^{-1}$)	10	10	10	10	(Zajac and Gordon 1989)
L_0 (cm)	5.10	5.88	4.40	6.83	(Arnold, Ward et al. 2010)
T_s (cm)	40.1	38.2	28.2	24.1	(Arnold, Ward et al. 2010)
T_{strain} (%)	10	10	11	9	(Farris, Hicks et al. 2014)
τ_{act}	0.01	0.01	0.01	0.01	(Winters and Stark 1988)
τ_{deact}	0.04	0.04	0.04	0.04	(Winters and Stark 1988)

This base model was scaled to each subject's anthropometry using marker data from static trials as per recommended scaling best practices. An inverse kinematics solution was found using the marker data from motion capture to identify the joint kinematics, and inverse dynamics was used to determine the time-varying joint moments. Verification of the models and analyses was done by comparing inverse

kinematics, moments, and powers from the same subjects previously reported by Collins et al. (Collins, Wiggin et al. 2015). All data were evaluated over four to seven consecutive steps beginning with heel strike. Heel strike was defined to be the instant when the calcaneus marker went from positive to negative velocity and toe off was defined as the instant when the calcaneus marker went from negative to positive velocity (Zeni, Richards et al. 2008). By this definition, heel strike and toe off typically occurred within one frame of ground reaction force gait event determinants on the treadmill. Kinematics were then prescribed to the models by splining the inverse kinematics solution to a scaled model creating a new model for each motion trial.

2.3 Simulation

The processed and tuned EMG data were then used to drive forward dynamic simulations of the muscles on the previously scaled models with constrained kinematics. Joint angles from constrained kinematics were used to define lengths and velocities of the muscle-tendon units allowing the EMG activations to drive the resultant muscle-level dynamics. Constraining kinematics during the forward simulation controls the MTU lengths allowing the EMG to manipulate the dynamics of the muscle fascicles and tendons. This simulation resulted in muscle states including fiber and tendon forces, lengths, and velocities. These resultant muscle states provided inputs to an energetic model to simulate muscle metabolic power (Umberger, Gerritsen et al. 2003, Umberger 2010). This model estimates the

metabolic power of the muscles by accounting for the heat rate contributions of several different sources.

$$\dot{E} = Basal + \sum_{muscles} (\dot{h}_A + \dot{h}_M + \dot{h}_{SL} + w_{CE}) \quad (1)$$

Equation 1 shows the calculation of metabolic power from the energetic model which is composed of five heat rates. *Basal* is the basal heat rate of the body and is independent of muscle. This value was set to zero for all calculations to observe only muscle-level effects. Activation \dot{h}_A , maintenance \dot{h}_M , shortening/lengthening \dot{h}_{SL} , and mechanical work w_{CE} heat rates are all calculated based on the activation, force, and fiber length and velocity states of the muscles (Umberger, Gerritsen et al. 2003, Umberger 2010).

2.4 Analysis

Joint-level kinematics, dynamics, and powers were first compared to previously published values (Collins, Wiggin et al. 2015) which verified the model and confirmed that there were minimal differences between the no exoskeleton and exoskeleton no spring conditions. Each simulated step within each condition was accounted for in the reported averages and all metrics were normalized before a combined average was taken. Fiber forces and lengths were normalized to maximum isometric force and optimized fiber length, respectively, as defined by the model. Shortening velocity was normalized to optimal fiber lengths per second with the model defining maximum velocity as ten optimal fiber lengths per second. Force

generation ability (or force per unit activation) (Equation 2), was also calculated for each muscle.

$$\text{Force generation ability} = \frac{F_{act}}{F_{max} \cdot Act} = f_{FL}(L_{CE}) \cdot f_{FV}(v_{CE}) \quad (2)$$

CHAPTER 3: RESULTS

3.1 Joint-level Verification and Results

Joint level analyses of kinematics, moments, and powers predicted by our simulations are consistent with previously published values (Collins, Wiggin et al. 2015) (Fig. 3.1). Limited errors seen in these results are potentially caused using different steps during simulations. Differences in power may also be resultant of errors in kinematics. The difference between the biological moment production in the exoskeleton no spring and spring conditions represents spring force provided by the exoskeleton during stance (0-60% stride); limited differences among all conditions were seen during swing, as expected (Fig. 3.2). Simulated ankle kinematics (left), dynamics (middle), and power (right) comparing our simulation (blue) to Collins et al. 2015 (black).

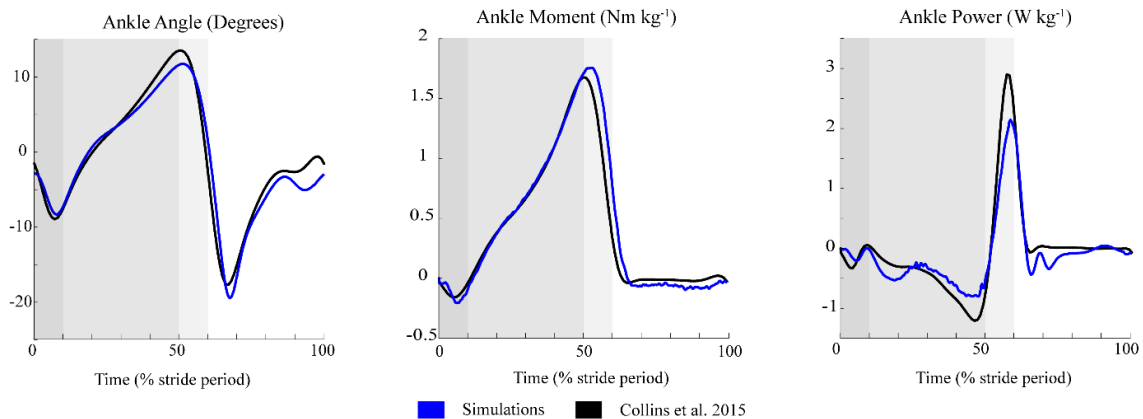


Figure 3.1: Simulated ankle kinematics, dynamics, and power.

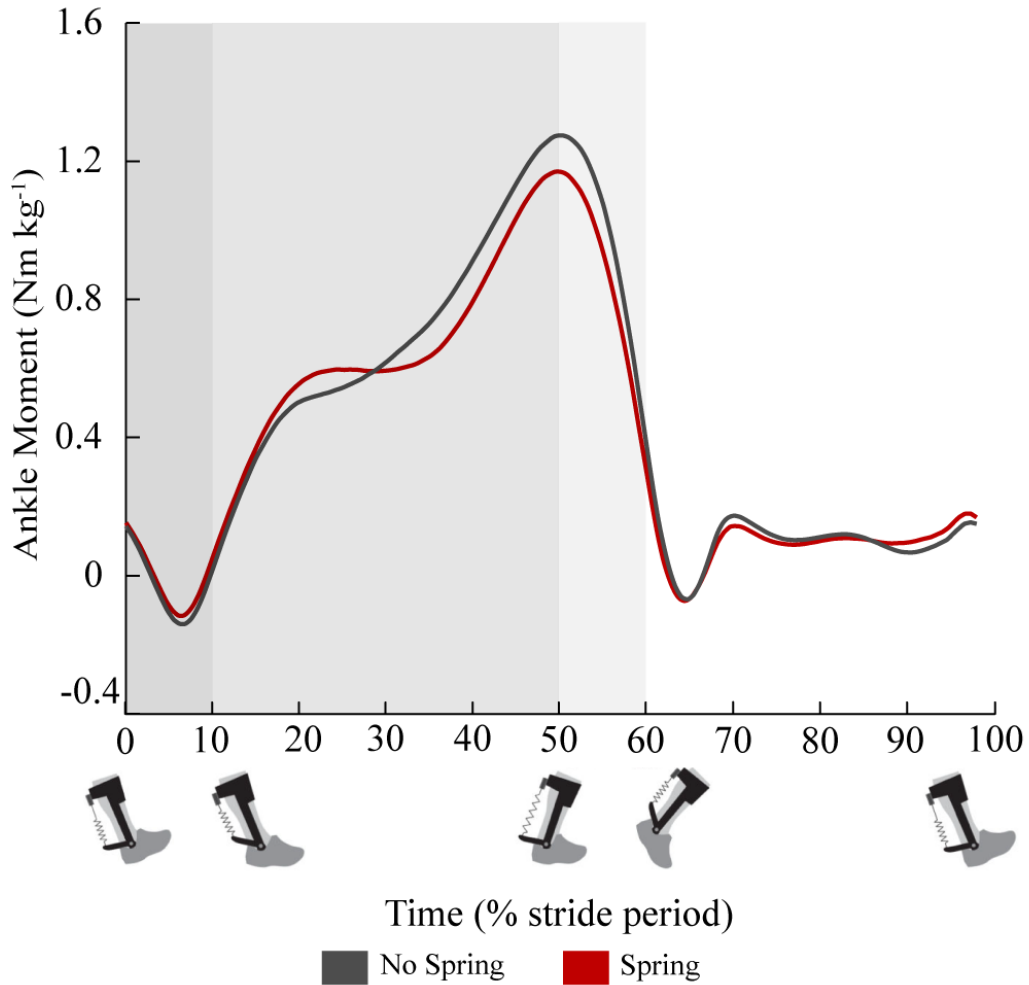


Figure 3.2: Average ankle dynamics verification.

Ankle kinematics remain similar through early stance and begin to shift to a more plantarflexed position during mid stance (Fig 3.3). Kinematics represented as average over stride where angle is measured in degrees. Positive is indicative of ankle plantarflexion and negative is ankle dorsiflexion. Peak dorsiflexion angle is reduced at heel off during the start of late stance while peak plantarflexion angle early in swing

phase is increased for the spring condition. This leaves the ankle in a generally more plantarflexed position for most of stride.

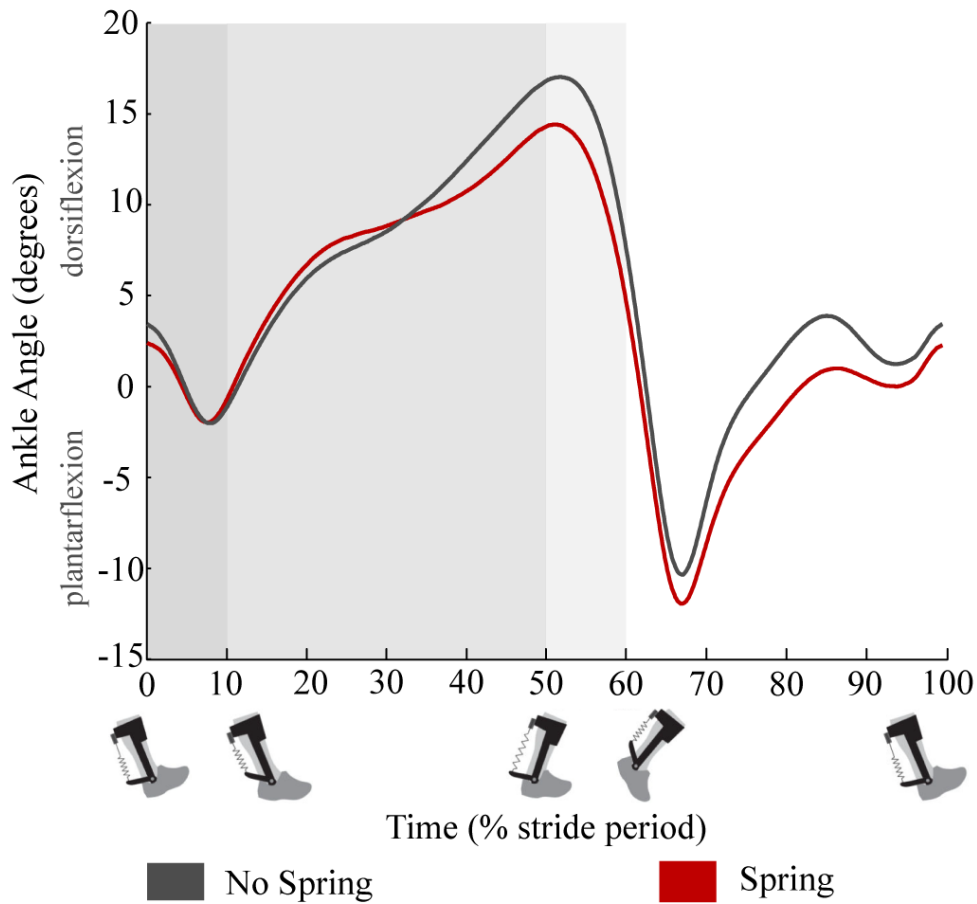


Figure 3.3: Altered ankle kinematics

3.2 Muscle-level Results

Overall, force and activation were reduced for plantarflexors while operating fiber lengths tended to increase during stance. Force generating ability was not majorly affected in the spring condition but metabolic costs were reduced. The SOL and MG responded to assistance similarly while the LG tended to have opposite

effects. Differences were also observed at the transition from mid to late stance in several of the muscle states including force generation ability, fiber length, and metabolic cost.

Force and Activation: The SOL and MG produced less force, 9.0% and 16.7% respectively, during stance but the LG generated 14.7% higher forces with the addition of spring assistance (Fig 3.4). Activation showed a similar trend in that the SOL and MG showed a 7.8% and 17.1% reduction, respectively, and the LG was 16.3% more activated than without spring assistance (Fig. 3.5). The average force generation ability of the SOL and MG increased by 1.6% and 1.9% respectively during stance and the force generation ability of the LG was reduced by 4.0% with assistance (Fig. 3.6). At the transition from mid to late stance, both the SOL and MG shifted from improved force generation ability (1.7% and 1.8% increase) to reduced force generation ability (4.8% and 1.8% decrease) during spring assistance.

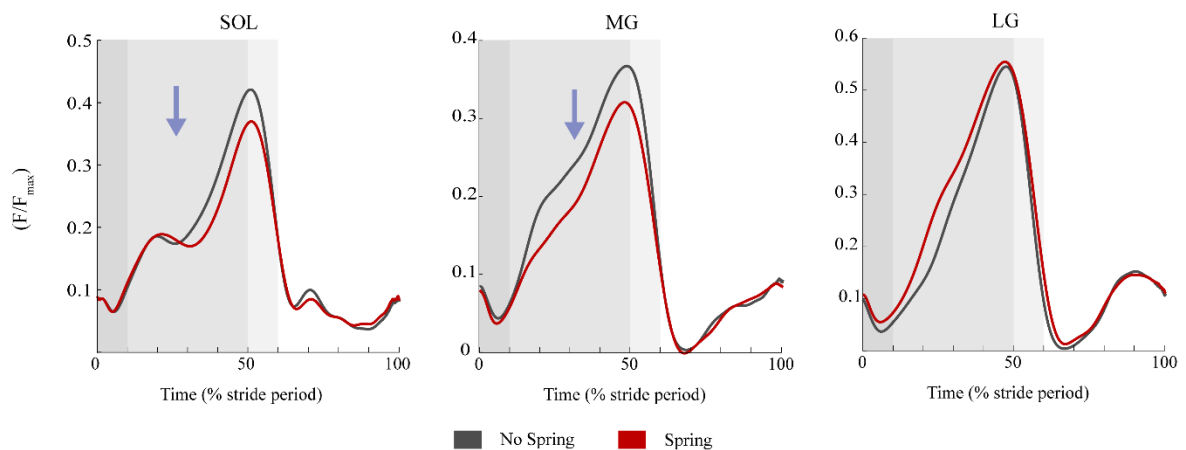


Figure 3.4: Normalized ankle plantarflexor force.

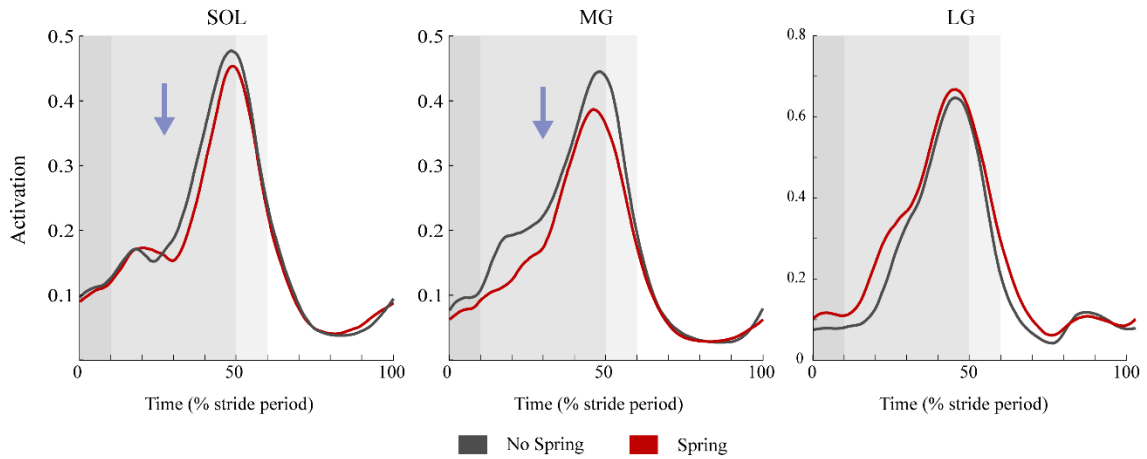


Figure 3.5: Activation of plantarflexor muscles.

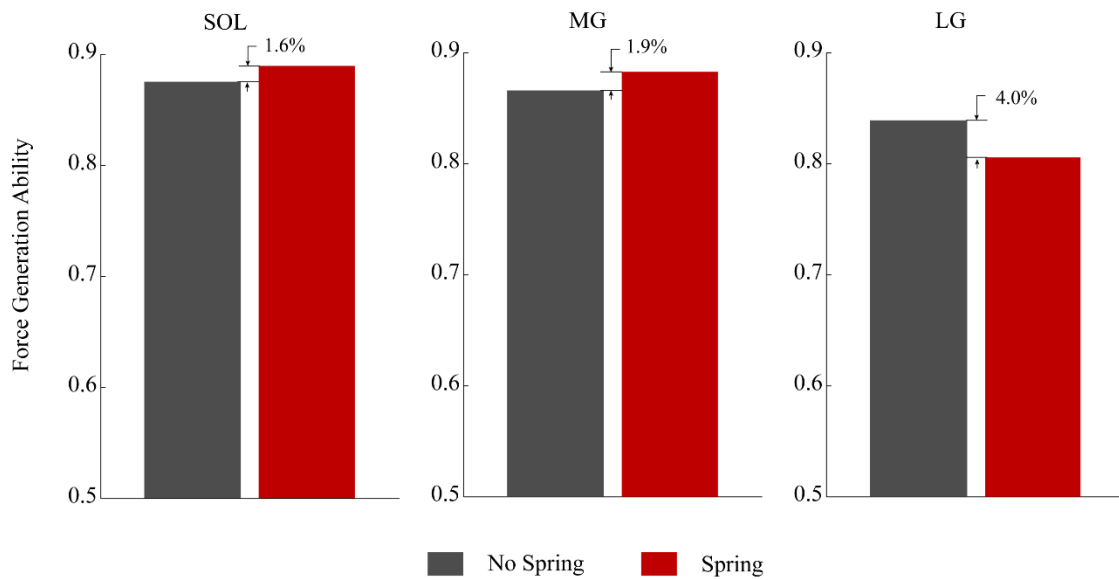


Figure 3.6: Force generation ability of plantarflexor muscles.

Fiber Length: The SOL average operating fiber length was not substantially increased (0.1% increase) but peak fiber length during stance was increased by 1.6%

(Fig 3.7). During mid stance, average fiber length of the SOL was increased by 0.7% but was decreased by 1.5% during late stance. The MG operated at 2.5% higher average operating fiber length during stance and peak operating fiber length during stance was increased by 4.2%. The LG operated at a lower average operating fiber length consistently throughout stance (2.9%).

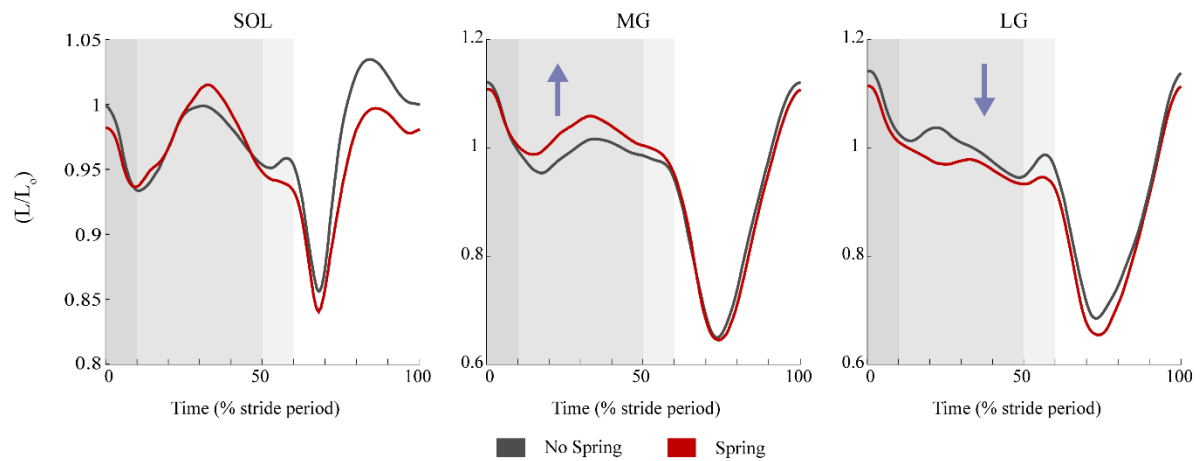


Figure 3.7: Normalized fiber length of plantarflexor muscles.

Metabolic Cost: The SOL and MG consumed 6.1% and 18.7% less metabolic energy respectively with the assistance of the spring while the LG cost 11.1% more metabolic energy during stance (Fig 3.8). The summed panel from bottom to top is SOL, MG, and LG contributions respectively (Fig. 3.8). The net metabolic consumption of plantarflexor muscles decreased by 6.9% for the spring assisted walking condition (Fig 3.8). The total metabolic saving of the plantarflexor muscles

was $.075 \text{ W kg}^{-1}$, which accounts for approximately 27% of the total metabolic savings previously found (Collins, Wiggin et al. 2015).

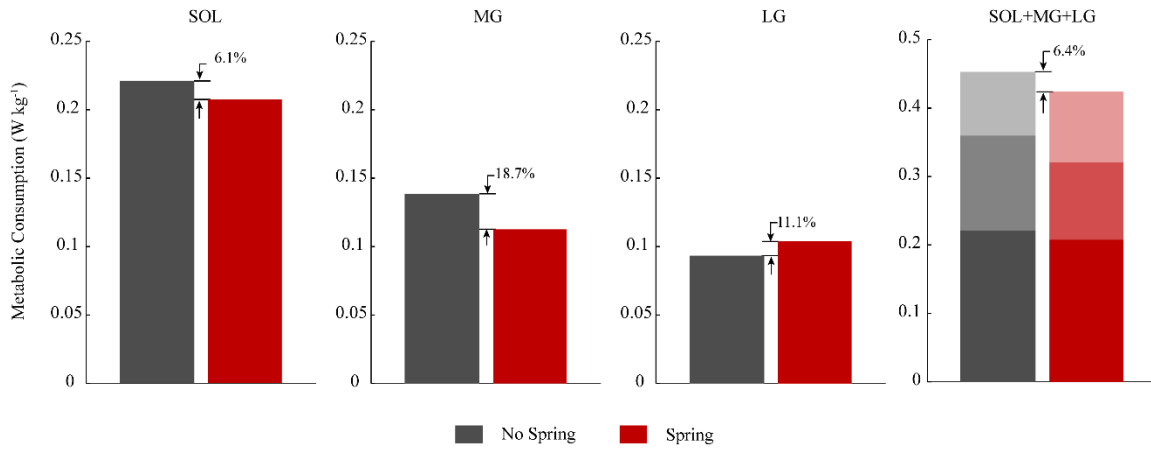


Figure 3.8: Metabolic energy consumption.

CHAPTER 4: DISCUSSION

4.1 Summary

We employed multi-joint models to produce forward simulations driven by experimental data to investigate the effect well-tuned assistance has on underlying plantarflexor muscles. We observed detuned muscle mechanics during mid stance and large reductions in activation and force during mid and late stance. This suggests that the exoskeleton robs the tendon of passive stored energy in mid stance. This causes reduced tendon stretch due to unloading of the MTU resulting in longer muscle fiber lengths. Contractile element lengthening could be related to observed alterations in kinematic pattern. Force generating ability of the plantarflexors was not substantially affected by these changes. The combination of force reduction and constant force generation ability results in decreased metabolic consumption for the plantarflexors during assisted walking.

4.2 Discussion

Operating fiber lengths of plantarflexors were increased during stance phase, which is consistent with predictions by previous simulations (Sawicki and Khan 2015). Altered kinematics were likely related to the SOL and MG fiber lengths operating above optimal fiber length during mid stance. This places the muscle operating point on the descending limb of the force-length relationship, which is thought to be unusual in normal unassisted locomotion because it is considered an unstable position for the muscle (Allinger, Epstein et al. 1996). The contractile element in muscle produces less active force above optimal fiber length and passive

forces begin to increase. Passive forces increase markedly as stretch increases above the optimal point causing a local minimum to occur just above optimal fiber length. Muscles operating above optimal fiber length are also at a higher risk of injury (Morgan 1990). To avoid this position, kinematic patterns may be altered. Our data shows that lengthening of muscle fibers above optimal fiber length occurs at the same time in the gait cycle as when the ankle kinematics begin to diverge from the no spring condition (c.f. Fig 3.5, normalized lengths greater than 1).

Despite altered kinematics, the force generation ability – which includes contributions of the force-length-velocity behavior of muscle – is maintained. Force generation ability is a metric that is often used to evaluate results of muscle states from simulations (Arnold, Hamner et al. 2013, Farris, Hicks et al. 2014). Implied by its name, this unitless value reveals the maximum force-producing capability of a muscle. This simple metric is valuable because it gives insight into the force-length and force-velocity relationships that are difficult to otherwise estimate and measure.

Assisted walking achieved a 6.9% decrease in plantarflexor metabolic cost which follows the trend of 7.2% whole-body metabolic reduction previously reported (Collins, Wiggin et al. 2015). Although these directly assisted muscles do reflect a metabolic reduction, only 5.1 W or 0.075 W kg^{-1} was saved across both legs, which does not account fully account for the net reduction of approximately 0.2 W kg^{-1} previously reported. The previous study reported alterations in knee dynamics during assisted walking as well. This suggests that proximal joints may also contribute to the decrease in whole-body metabolic cost as predicted in a previous simplified, idealized

exoskeleton simulation (Uchida, Seth et al. 2016). This effect was seen in a study in which a powered ankle exoskeleton device was shown to reduce metabolic cost below that of unassisted walking. Joint-level analysis revealed a mechanical power reduction at the ankle, knee, and hip joints (Mooney and Herr 2016). The work linkage between joints found in this study supports the results presented here that only a portion of the observed total metabolic reduction was found. Another study simulated energetics of muscles that cross the ankle, knee, and hip joints during unilateral exoskeleton-assisted walking and revealed that the contralateral vastus medialis metabolic rate followed the same trend as whole body metabolic measurements (Jackson, Dembia et al. 2017). These studies provide evidence that factors up the change may play a role in reducing metabolic expenditure during assisted walking.

The biarticular gastrocnemius heads react to ankle assistance in opposite ways despite their similar geometry. The MG responded similarly to the uniarticular SOL which reacted with increased operating fiber length and reduced force and activation as predicted by previous simplified models (Sawicki and Khan 2015) however, the LG was not impacted as markedly and reacted oppositely to assistance. The MG demonstrated reduced muscle activation and force and operated at a higher average fiber length during stance, resulting in higher force generation ability and increased metabolic efficiency. The LG had slightly increased force and activation while operating at a lower average fiber which reduced force generation ability and increased metabolic consumption. This may be explained by differing roles that the MG and LG play during walking. The exoskeleton device locked the ankle in the

frontal plane, which may have added stability to the ankle. Additional stability could have the effect of reducing muscle activation due to a muscle no longer being required to provide stabilization or it could have the effect of increasing due to a muscle not being constrained by having to account for stabilization.

4.3 Limitations

Although models were scaled to anthropometric data of static trials to generate individualized models for analysis, they are not fully subject specific. Muscle model parameters such as maximum isometric force were based on averages from literature. Lack of MVC data also affected the scaling of EMG data used to drive the forward simulation resulting in the gain-tuning process. Tuning EMG data without MVC data was done using the same process of comparing inverse and forward run solutions as a previous hopping study (Farris, Hicks et al. 2014). A single gain parameter was tuned for each subject and applied to all muscles. This approach assumes that relative proportions of plantarflexor muscles are do not have large variations for healthy individuals which has been shown to be a reasonable assumption for healthy individuals (Handsfield, Meyer et al. 2014). This approach was used to minimize the number of optimized parameters and preserve the relative measured activations. Another approach would be to optimize the gain for each muscle using MVC data as was used in a similar study (Jackson, Dembia et al. 2017). One advantage of this approach would be that it can adjust for variations that can occur due to surface EMG electrodes placement. Furthermore, no scaling of muscle paths (and thus, moment

arms) was performed which may affect subject-specific behavior. This approach isolates the effects of muscle activation and kinematics on the observed dynamics.

Muscle activation data were collected using surface EMG placed underneath the exoskeleton which was susceptible to movement artifact and low frequency spikes. Movement artifact can occur if the wires are pulled during data collection due to not enough slack being provided to them. Low frequency spikes were prevalent in the muscle activation data, likely due to the recoil of the spring hitting the surface EMG electrode during propulsion. Movement artifact and low frequency spikes were not able to be completely removed from the data using filtering techniques.

The simulation was sensitive to the driving experimental EMG noise motivating selecting only portions of the data set with at least three consecutive steps with no low frequency spikes and minimal movement artifact. Thus, only four of the nine subjects walking at three out of the seven conditions were used for analysis. Although the no exoskeleton condition for these subjects was used to tune the EMG gain, only the no spring and “sweet spot” spring stiffness conditions were evaluated at the muscle-level. These two conditions were chosen for analysis because these conditions had the same marker set locations, whereas the no exoskeleton marker set was in a different location.

Simulations of each condition were run as consecutive steps as opposed to averaging the response, to include step to step variation. Driving simulations with average step data would provide more stable simulations, but may obscure variations in coupled EMG and kinematic changes that occur in a single step. Models and

simulations are not particularly well equipped to determine the effects of step to step perturbations due to initial conditions and time for the simulation to reach equilibrium. To reduce this effect, simulations were started before heel strike of the first analyzed step with ample time for the model to reach an equilibrium of operating states.

CHAPTER 5: CONCLUSION

5.1 Conclusion

In conclusion, our simulations show reduced force production during stance resulting from passive exoskeleton assistance. This simulation study reveals increased fiber lengths in unloaded muscle-tendon units occurring simultaneously with altered kinematics. During assisted walking, metabolic consumption of the underlying plantarflexor muscles was reduced however this local muscle reduction does not account for the whole-body metabolic reduction previously reported by Collins et al (2015). This simulation also demonstrated that muscles with similar geometry such as the MG and LG can respond differently due to different roles during gait. This confirms that well-tuned assistance to muscle-tendon units can provide benefits to the local muscles and further demonstrates the importance of discovering the muscle-level reactions to stimulations, perturbances, disturbances, alterations, on underlying muscles. Our hypothesis of improved local metabolic efficiency despite increased operating fiber lengths was supported and may help to further explain the apparent trade-off predicted by a simplified model (Sawicki and Khan 2015).

5.2 Future Work

To experimentally verify the predictions made by this model, ultrasound imaging measurements of SOL *in vivo* during exoskeleton-assisted walking could be collected. This would allow for more accurate fiber lengths as well as allow for a more accurate and individualized approach for studying muscle mechanics. If space permits or in a follow-up study, experimentally measuring the gastrocnemius fiber

lengths during assisted walking could further evaluate the predictions of our model. Confirmation of predictions made by this simulation would also give more confidence in future models that may aim to replicate this experimental simulation framework.

As we age, our muscles get weaker and we operate at shorter fiber lengths due to tendon stretch (Franz 2016). These aging effects are the opposite of the effects seen for this device. A similar experiment to that done by Collins et al. could be performed with elderly subject to determine if this device could have beneficial results for this population. Exoskeletons have been shown to be feasible for elderly with regards to difficulty of use, comfort, muscle and overall fatigue, and balance (Galle, Derave et al. 2017).

Whether this device should be considered a rehabilitative or assistive device also remains unclear. A rehabilitative or training study could be performed to determine if walking in propulsion-assisting devices has lasting effects on underlying MTUs. An experiment could potentially be run in which subjects walked in a similar device that resisted instead of assisted plantarflexion.

REFERENCES

- Allinger, T. L., M. Epstein and W. Herzog (1996). "Stability of muscle fibers on the descending limb of the force-length relation. A theoretical consideration." J Biomech **29**(5): 627-633.
- Arnold, E. M., S. R. Hamner, A. Seth, M. Millard and S. L. Delp (2013). "How muscle fiber lengths and velocities affect muscle force generation as humans walk and run at different speeds." J Exp Biol **216**(Pt 11): 2150-2160.
- Arnold, E. M., S. R. Ward, R. L. Lieber and S. L. Delp (2010). "A model of the lower limb for analysis of human movement." Ann Biomed Eng **38**(2): 269-279.
- Banala, S. K., S. H. Kim, S. K. Agrawal and J. P. Scholz (2009). "Robot assisted gait training with active leg exoskeleton (ALEX)." IEEE Trans Neural Syst Rehabil Eng **17**(1): 2-8.
- Cherry, M. S., S. Kota, A. Young and D. P. Ferris (2016). "Running With an Elastic Lower Limb Exoskeleton." J Appl Biomech **32**(3): 269-277.
- Collins, S. H., M. B. Wiggin and G. S. Sawicki (2015). "Reducing the energy cost of human walking using an unpowered exoskeleton." Nature **522**(7555): 212-215.
- Delp, S. L., F. C. Anderson, A. S. Arnold, P. Loan, A. Habib, C. T. John, E. Guendelman and D. G. Thelen (2007). "OpenSim: open-source software to create and analyze dynamic simulations of movement." IEEE Trans Biomed Eng **54**(11): 1940-1950.

Donelan, J. M., Q. Li, V. Naing, J. A. Hoffer, D. J. Weber and A. D. Kuo (2008). "Biomechanical energy harvesting: generating electricity during walking with minimal user effort." Science **319**(5864): 807-810.

Elliott, G., G. S. Sawicki, A. Marecki and H. Herr (2013). "The biomechanics and energetics of human running using an elastic knee exoskeleton." IEEE Int Conf Rehabil Robot **2013**: 6650418.

Farris, D. J., J. L. Hicks, S. L. Delp and G. S. Sawicki (2014). "Musculoskeletal modelling deconstructs the paradoxical effects of elastic ankle exoskeletons on plantar-flexor mechanics and energetics during hopping." J Exp Biol **217**(Pt 22): 4018-4028.

Farris, D. J., B. D. Robertson and G. S. Sawicki (2013). "Elastic ankle exoskeletons reduce soleus muscle force but not work in human hopping." J Appl Physiol (1985) **115**(5): 579-585.

Farris, D. J. and G. S. Sawicki (2012). "Linking the mechanics and energetics of hopping with elastic ankle exoskeletons." J Appl Physiol (1985) **113**(12): 1862-1872.

Franz, J. R. (2016). "The Age-Associated Reduction in Propulsive Power Generation in Walking." Exerc Sport Sci Rev **44**(4): 129-136.

Galle, S., W. Derave, F. Bossuyt, P. Calders, P. Malcolm and D. De Clercq (2017). "Exoskeleton plantarflexion assistance for elderly." Gait Posture **52**: 183-188.

Grabowski, A. M. and H. M. Herr (2009). "Leg exoskeleton reduces the metabolic cost of human hopping." J Appl Physiol (1985) **107**(3): 670-678.

Gregorczyk, K. N., L. Hasselquist, J. M. Schiffman, C. K. Bensek, J. P. Obusek and D. J. Gutekunst (2010). "Effects of a lower-body exoskeleton device on metabolic cost and gait biomechanics during load carriage." Ergonomics **53**(10): 1263-1275.

Handsfield, G. G., C. H. Meyer, J. M. Hart, M. F. Abel and S. S. Blemker (2014). "Relationships of 35 lower limb muscles to height and body mass quantified using MRI." J Biomech **47**(3): 631-638.

Jackson, R. W., C. L. Dembia, S. L. Delp and S. H. Collins (2017). "Muscle-tendon mechanics explain unexpected effects of exoskeleton assistance on metabolic rate during walking." J Exp Biol.

Knaggs, J. D., K. A. Larkin and T. M. Manini (2011). "Metabolic cost of daily activities and effect of mobility impairment in older adults." J Am Geriatr Soc **59**(11): 2118-2123.

Malcolm, P., W. Derave, S. Galle and D. De Clercq (2013). "A simple exoskeleton that assists plantarflexion can reduce the metabolic cost of human walking." PLoS One **8**(2): e56137.

Martin, P. E., D. E. Rothstein and D. D. Larish (1992). "Effects of age and physical activity status on the speed-aerobic demand relationship of walking." J Appl Physiol (1985) **73**(1): 200-206.

Mooney, L. M. and H. M. Herr (2016). "Biomechanical walking mechanisms underlying the metabolic reduction caused by an autonomous exoskeleton." J Neuroeng Rehabil **13**: 4.

Mooney, L. M., E. J. Rouse and H. M. Herr (2014). "Autonomous exoskeleton reduces metabolic cost of human walking." J Neuroeng Rehabil **11**: 151.

Morgan, D. L. (1990). "New insights into the behavior of muscle during active lengthening." Biophys J **57**(2): 209-221.

Norris, J. A., K. P. Granata, M. R. Mitros, E. M. Byrne and A. P. Marsh (2007). "Effect of augmented plantarflexion power on preferred walking speed and economy in young and older adults." Gait Posture **25**(4): 620-627.

Platts, M. M., D. Rafferty and L. Paul (2006). "Metabolic cost of over ground gait in younger stroke patients and healthy controls." Med Sci Sports Exerc **38**(6): 1041-1046.

Sawicki, G. and N. Khan (2015). "A simple model to estimate plantarflexor muscle-tendon mechanics and energetics during walking with elastic ankle exoskeletons." IEEE Trans Biomed Eng.

Uchida, T. K., A. Seth, S. Pouya, C. L. Dembia, J. L. Hicks and S. L. Delp (2016). "Simulating Ideal Assistive Devices to Reduce the Metabolic Cost of Running." PLoS One **11**(9): e0163417.

Umberger, B. R. (2010). "Stance and swing phase costs in human walking." J R Soc Interface **7**(50): 1329-1340.

Umberger, B. R., K. G. Gerritsen and P. E. Martin (2003). "A model of human muscle energy expenditure." Comput Methods Biomech Biomed Engin **6**(2): 99-111.

van Dijk, W., H. van der Kooij and E. Hekman (2011). "A passive exoskeleton with artificial tendons: design and experimental evaluation." IEEE Int Conf Rehabil Robot **2011**: 5975470.

Westerterp, K. R. (2013). "Physical activity and physical activity induced energy expenditure in humans: measurement, determinants, and effects." Front Physiol **4**: 90.

Winters, J. M. and L. Stark (1988). "Estimated mechanical properties of synergistic muscles involved in movements of a variety of human joints." J Biomech **21**(12): 1027-1041.

Zajac, F. E. and M. E. Gordon (1989). "Determining muscle's force and action in multi-articular movement." Exerc Sport Sci Rev **17**: 187-230.

Zeni, J. A., Jr., J. G. Richards and J. S. Higginson (2008). "Two simple methods for determining gait events during treadmill and overground walking using kinematic data." Gait Posture **27**(4): 710-714.

APPENDIX

Appendix A

Table A1: Average normalized fiber length for no spring condition

Normalized fiber length	Early	Mid	Late	Stance	Stride
MG	1.062	0.990	0.971	0.999	0.943
LG	1.089	0.999	0.972	1.010	0.948
SOL	0.967	0.973	0.954	0.969	0.972
TA	0.756	0.785	0.748	0.774	0.803

Table A2: Average normalized fiber length for spring condition

Normalized fiber length	Early	Mid	Late	Stance	Stride
MG	1.059	1.024	0.986	1.024	0.952
LG	1.064	0.970	0.939	0.981	0.919
SOL	0.958	0.980	0.941	0.970	0.960
TA	0.772	0.793	0.783	0.788	0.822

Table A3: Average activation for no spring condition

Activation	Early	Mid	Late	Stance	Stride
MG	0.09	0.27	0.32	0.25	0.17
LG	0.08	0.36	0.34	0.31	0.22
SOL	0.11	0.26	0.37	0.25	0.18
TA	0.71	0.17	0.13	0.25	0.27

Table A4: Average activation for spring condition

Activation	Early	Mid	Late	Stance	Stride
MG	0.08	0.22	0.27	0.20	0.14
LG	0.11	0.41	0.40	0.36	0.25
SOL	0.11	0.23	0.35	0.23	0.17
TA	0.67	0.16	0.11	0.23	0.25

Table A5: Average metabolic cost for no spring condition

Metabolic Cost (W)	Early	Mid	Late	Stance	Stride
MG	10.0	15.6	22.0	15.7	12.8
LG	3.7	13.2	6.8	10.6	7.1
SOL	18.8	25.7	28.9	25.0	18.9
TA	22.4	4.0	2.07	6.8	8.6

Table A6: Average metabolic cost for spring condition

Metabolic Cost (W)	Early	Mid	Late	Stance	Stride
MG	7.3	13.4	15.7	12.8	8.8
LG	5.2	14.1	9.1	11.7	7.9
SOL	16.0	24.0	29.2	23.5	17.6
TA	21.8	3.2	1.3	6.0	7.8

Table A7: Average normalized fiber force for no spring condition

Normalized Fiber Force	Early	Mid	Late	Stance	Stride
MG	0.06	0.24	0.26	0.21	0.15
LG	0.06	0.29	0.32	0.26	0.19
SOL	0.08	0.23	0.34	0.22	0.16
TA	0.44	0.18	0.20	0.22	0.21

Table A8: Average normalized fiber force for spring condition

Normalized Fiber Force	Early	Mid	Late	Stance	Stride
MG	0.05	0.20	0.22	0.18	0.12
LG	0.07	0.34	0.36	0.30	0.21
SOL	0.08	0.21	0.31	0.20	0.15
TA	0.39	0.15	0.18	0.20	0.19

Table A9: Average force generation ability for no spring condition

Force Generation Ability	Early	Mid	Late	Stance	Stride
MG	0.64	0.91	0.79	0.85	1.04
LG	0.73	0.98	1.02	0.94	1.01
SOL	0.75	0.89	0.87	0.87	0.93
TA	0.73	0.85	0.90	0.84	0.82

Table A10: Average force generation ability for spring condition

Force Generation Ability	Early	Mid	Late	Stance	Stride
MG	0.73	0.98	0.78	0.90	1.03
LG	0.72	0.86	0.85	0.83	0.91
SOL	0.78	0.96	0.89	0.92	0.95
TA	0.75	0.82	1.04	0.85	0.84